PERGAMON

International Journal of Heat and Mass Transfer 45 (2002) 4823–4829

International Journal of HEAT and MASS TRANSFER

www.elsevier.com/locate/ijhmt

Boiling heat transfer characteristics of R-113 in a vertical small diameter tube under natural circulation condition

Chowdhury Feroz Md [a,*], Fumito Kaminaga [b]

[a] Department of Mechanical Engineering, Bangladesh University of Engineering and Technology, Dhaka 1000, Bangladesh
[b] Department of Mechanical Engineering, Ibaraki University, 4-12-1 Nakanarusawa, Hitachi 316-8511, Japan

Received 2 February 2002; received in revised form 30 April 2002

Abstract

Boiling heat transfer characteristics of freon R-113 are experimentally investigated in a vertical small diameter tube, $D = 1.45$ mm and $L = 100$ mm at a wide pressure range of 19–269 kPa under natural circulation condition. Except the entrance region of the test section, the flow regime is annular in view of the measured vapor flux. The pool boiling correlations of Stephan and Abdelsalam and McNelly equally well predict the experimental data within an error of $\pm 20\%$. No enhancement of heat transfer coefficient is obtained although D/B is less than 1.5, which differs from the finding of Klimenko.
© 2002 Published by Elsevier Science Ltd.

Keywords: Two-phase flow; Heat transfer enhancement; Small diameter tube; Low pressure; Natural circulation

1. Introduction

Confined device cooling incorporates several small and short coolant passages similar to those described in this paper. Refrigerants may be the preferred coolant since fluorocarbons possess high dielectric strength, boiled at moderate pressures with low saturation temperatures, and are compatible with materials commonly used in electrical and electronic devices.

Ishibashi and Nishikawa [1] presented the effect of fluid space on the boiling heat transfer using various annular working fluid space ranging from 0.57 to 83.5 mm at atmospheric and above atmospheric conditions and reported that the boiling heat transfer depends on the boiling space with ΔR as $h\alpha\Delta R^{-2/3}$. Since they used an annular boiling space in which the inner tube was heated and the outer one was adiabatic, the heat transfer characteristics and flow behavior of the working fluid in the space surrounded by the heated and unheated surfaces might be different from that in a single tube. Klimenko et al. [2] investigated the boiling heat transfer for a two-phase flow of nitrogen with the mass flux of 60–800 kg/m^2 s in stainless steel tubes having diameters of 4.0–18.9 mm and above atmospheric pressure in the range of 150–800 kPa. They reported that for channel diameters less than 1.5 times the Laplace constant, the deformation of vapor bubble results in an increase of boiling heat transfer. However, it is not clear that this finding can be applied to ordinary fluids or fluorocarbon refrigerants since the properties of ordinary fluids and refrigerants are much different from those of the cryogenics.

Flow boiling of fluorocarbon refrigerants has been investigated by many researchers. Wambsganss et al. [3] investigated the flow boiling of R-113 in a small diameter horizontal tube of 2.92 mm that corresponds to the diameter to Laplace constant ratio falling between 2.95 and 3.02, at a pressure range of 124–160 kPa with a mass flux varying from 50 to 300 kg/m^2 s. They reported that the majority of their boiling data has the plug and slug pattern flow regimes. The heat transfer trends show a dominance of the nucleation mechanism. The pool boiling correlation of Stephan and Abdelsalam [4] predicts the measured results well. Bowers and Mudawar [5]

* Corresponding author. Present address: Department of Mechanical Engineering, Ibaraki University, 4-12-1 Nakanarusawa, Hitachi 316-8511, Japan. Fax: +81-294-38-5047.

E-mail addresses: feroz@mech.ibaraki.ac.jp, feroz@me.buet.edu (C. Feroz Md).

0017-9310/02/$ - see front matter © 2002 Published by Elsevier Science Ltd.
PII: S0017-9310(02)00174-6

Nomenclature

B	Laplace constant, $\sqrt{\sigma/g(\rho_l-\rho_g)}$, m
D	inside diameter of tube, m
G	mass flux, kg/m^2 s
g	gravitational acceleration, m/s^2
h	heat transfer coefficient, W/m^2 K
h_{fg}	latent heat of vaporization, J/kg
j_g	superficial vapor velocity, $4qZ/(Dh_{fg}\rho_g)$, m/s
j_g^*	dimensionless vapor flux, $j_g\rho_g^{0.5}/[gD(\rho_g-\rho_l)]^{0.5}$
j_l	superficial liquid velocity, m/s
L	heated length, m
P	system pressure, kPa
q	heat flux, W/m^2
ΔR	gap size of annuli, m
T	temperature, K
x	quality
Z	axial distance from bottom of the heated tube, m
α	void fraction
δ	liquid film thickness, m
ρ	density, kg/m^3
μ	dynamic viscosity, Pa s
σ	surface tension, N/m

Subscripts

exp	experimental
g	vapor
l	liquid
s	saturated
w	wall

investigated flow boiling of R-113 in small diameter tubes of 0.51 and 2.54 mm, that correspond to the diameter to Laplace constant ratio of 0.52 and 2.6, at a pressure of 138 kPa with a mass flux ranging from 105 to 458 kg/m^2 s per one channel of 2.54 and 0.51 mm, respectively. They concluded that the heat transfer regime in their experimental range was the same as in ordinary pool boiling and the tube diameter effect on boiling heat transfer was negligible.

The findings mentioned above indicate that for the enhancement of boiling heat transfer the flow regime and behavior in a boiling passage should be taken into account besides the geometric parameter such as the ratio of tube diameter to Laplace constant. When R-113 is used as a working fluid in a thermosyphon or saturated cooling for electrical and electronic devices under a natural circulation condition, for very compact devices the heat transfer space should be as small as possible. So far the authors' know no comprehensive investigation has been performed on boiling heat transfer in a small diameter tube under a natural circulation condition. The purpose of our experimental investigation is to examine the boiling heat transfer regime in a small diameter tube below and above atmospheric pressures under natural circulation and to clarify the enhancement phenomenon by comparing the obtained results with established correlations.

2. Experimental apparatus and test procedure

A schematic diagram of the experimental apparatus is shown in Fig. 1 and dimensions of the test section and locations of the thermocouples are presented in Fig. 2. The test section (1) is made of stainless steel tube with

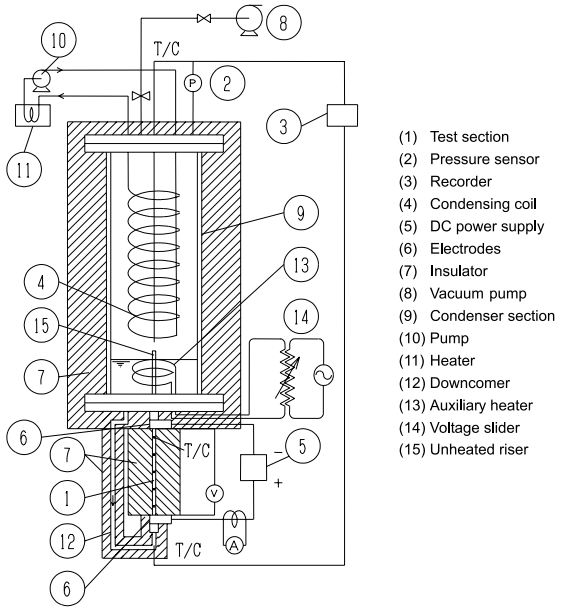

Fig. 1. Schematic diagram of the experimental apparatus.

inner diameter of 1.45 and a length of 100 mm. The condenser section is made of a glass cylinder (9) and a cooling coil (4) in which a water coolant with a constant temperature is circulated. The wall temperature of heating section is measured at five locations with 0.1 mm diameter chromel–alumel thermocouples placed on the outer surface of the tube. Two chromel–alumel sheathed thermocouples are inserted into the condenser section and the inlet of test section to measure the vapor temperature and the inlet liquid temperature, respectively. The system pressure is calculated from the saturated

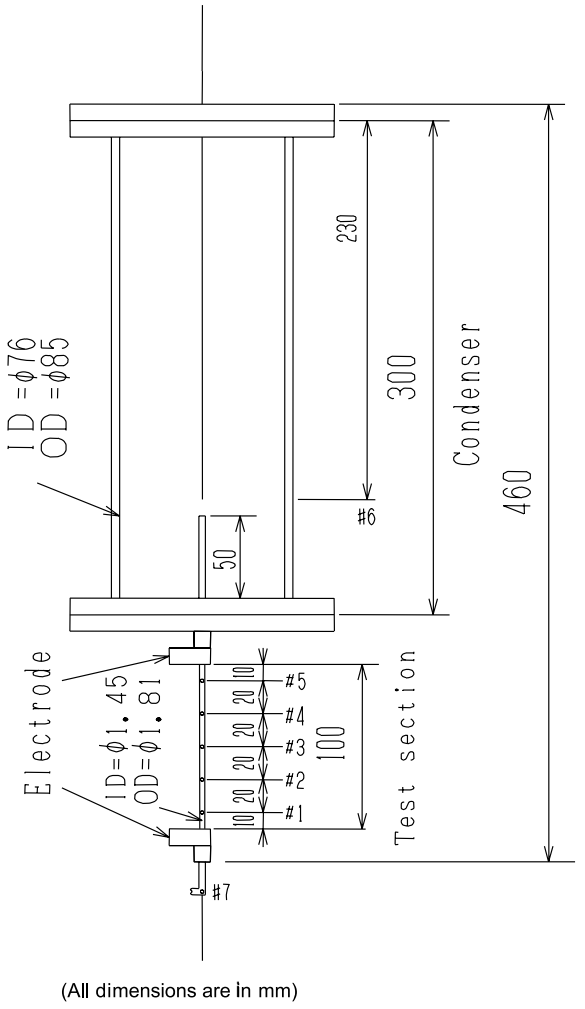

Fig. 2. Dimensions of the test section and locations of the thermocouples.

condition corresponding to the vapor temperature measured in the condensing section. All temperatures are measured by calibrated thermocouples and data acquisition system. Each thermocouple linked to the data acquisition system is calibrated by a platinum resistance thermometer with a constant water bath. An auxiliary heater (13) is installed at the bottom of condenser section to enable experimental condition to be saturated since the sub-cooling of inlet liquid gives a large hydraulic fluctuation like a geyser in the natural circulation condition. The condenser and the heated sections are connected with an unheated riser (15) of 50 mm long tube to prevent a back flow from the condenser directly to the test section. The downcomer (12) is a low resistance flow path made of an 8 mm inner diameter tube. Before the experiments, a resolved gas is degassed by the following manner. The working fluid is boiled

Table 1
Experimental parameter and their ranges

System pressure, P_s (kPa)	Heat flux, q (kW/m^2)	B (mm)	D/B
19	8.34–28.05	1.12	1.29
43	13.58–41.0	1.07	1.35
144	22.62–53.03	0.97	1.49
205	31.66–59.70	0.94	1.54
269	34.36–69.39	0.90	1.61

and condensed in the test rig for a few hours. After it is cooled down a dry type vacuum pump (8) is operated for a several minutes to remove the resolved gas accumulated in the upper part of the condenser section. This procedure is repeated three times. The test section is heated directly by passing DC current, and controlled by a adjustable DC power supply (5). Four hundred data per channel are scanned through a data acquisition system with a scan speed of 0.4 s per one datum. The experiments are conducted under natural circulation condition, and the experimental parameters and their ranges are indicated in Table 1. The experimental heat flux range covers up to near critical heat flux condition.

3. Experimental uncertainty

Temperature measurement uncertainty is estimated to be less than 0.2 °C considering thermocouple calibration errors. Uncertainty in evaluating the system pressure calculated from the saturated condition corresponding to the vapor temperature measured in the condensing section is less than 1%. The heat fluxes are determined from the electrical power, supplied to the test section through two electrodes located at the top and bottom ends, measured with an uncertainty of less than 2%.

4. Results and discussion

Fig. 3 presents the time traces of temperature measured at five elevations of the heated wall, inlet liquid, and vapor at a typical pressure of 43 kPa (since the temperature traces show the identical trends at other pressures). The temperatures are plotted for an arbitrary period of 160 s after the test rig has come to equilibrium. They show steady state traces without any fluctuation. At the other conditions, the temperature traces are almost similar to those shown in this figure. Since the thermocouples for the wall temperature measurement are attached on the outer surface of the test section, they can not detect high frequency phenomenon like bubble nucleation pertaining to a normal pool boiling. The stable wall temperature traces with small or negligible

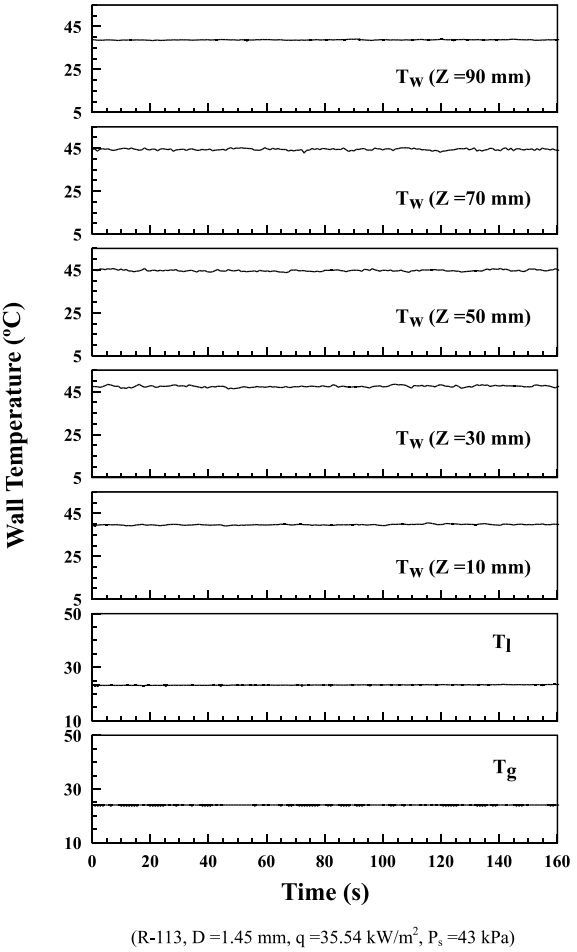

Fig. 3. Traces of heated wall, inlet liquid, and vapor temperatures.

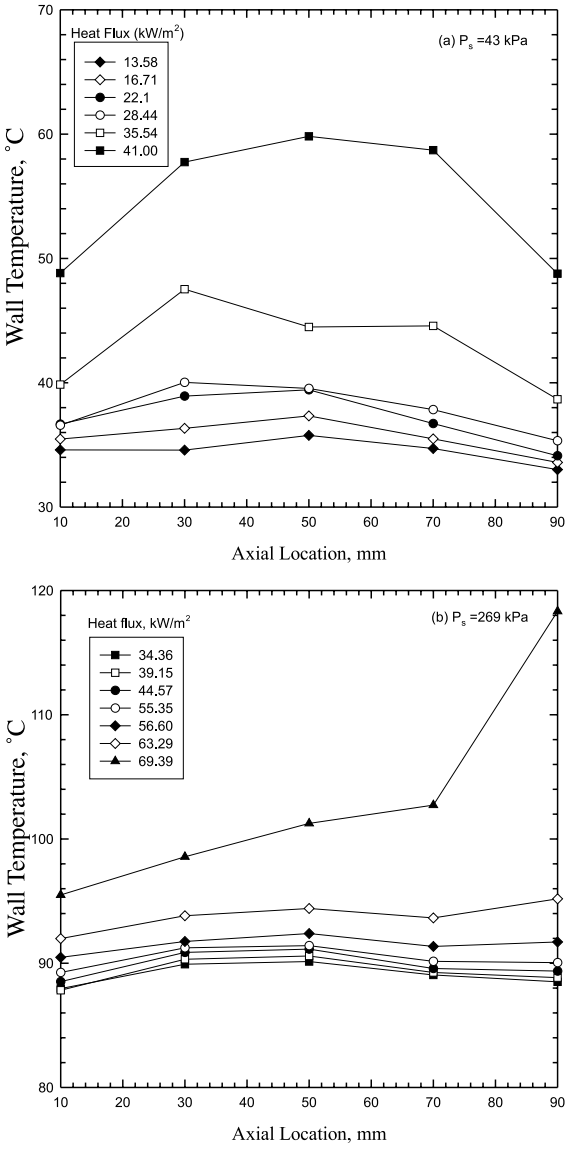

Fig. 4. Axial temperature profile of the heated wall.

amplitude in the fluctuation indicate a fully developed nucleate boiling or film evaporation.

Fig. 4(a) and (b) shows average wall temperature profiles on the heated section along the axial length from the bottom for system pressures below and above atmospheric, respectively. At a low system pressure of 43 kPa (below atmospheric) shown in Fig. 4(a), wall temperature profiles are almost flat below a heat flux of 30.0 kW/m^2. A peak of the wall temperature gradually shifts to the middle elevation of the test section with increasing heat flux. The reason of this shift has not been cleared yet, but at a low pressure the burnout is initiated around the middle elevation. At a high system pressure of 269 kPa (above atmospheric) shown in Fig. 4(b), wall temperature profiles monotonously increase at all elevations with increasing heat flux except at the highest heat flux condition with $Z = 90$ mm where temperature suddenly increases due to the burnout.

The representative wall temperature is calculated by averaging simply the measured ones with time, since the fluctuations are negligible as shown in Fig. 3. To obtain the heat transfer characteristics in the heated section the wall temperatures measured at five elevations are averaged to calculate the representative wall temperature. The boiling curves at different pressures shown in Fig. 5 are qualitatively similar to that for nucleate pool boiling, except the data at higher heat flux conditions which are very close to the critical.

The heated section in the present study is long enough compared with the diameter, $L/D = 69$, and the flow pattern must change along a heated length. The

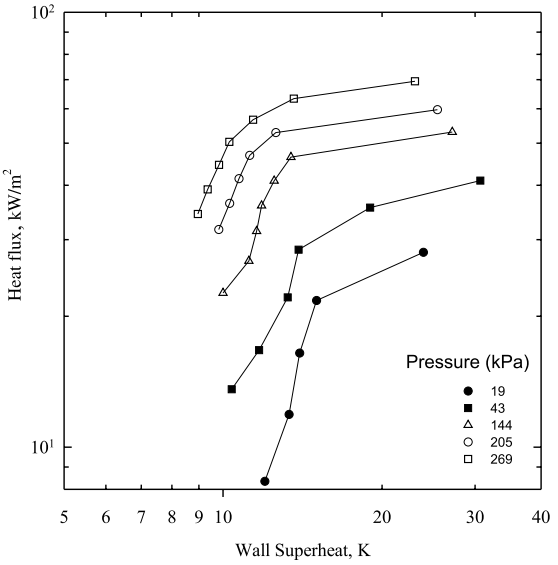

Fig. 5. Boiling curves.

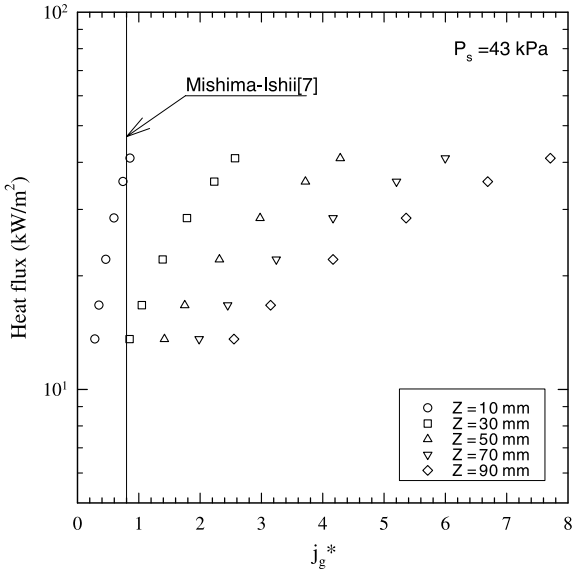

Fig. 6. Relationship between heat flux and dimensionless vapor flux.

flow pattern must be evaluated since the pattern might affect the heat transfer. Fig. 6 shows the relationship between the heat flux and dimensionless vapor flux at five different elevations at a pressure of 43 kPa. The same results exist at other pressures. Wallis [6] proposed that for the annular flow regime the dimensionless vapor flux is required to be greater than 0.9. Mishima and Ishii [7] also developed the following dimensionless vapor flux for the transition between churn-turbulent flow and annular flow regimes:

$$j_g^* = \sqrt{(\alpha - 0.11)} \tag{1}$$

This transition criterion was confirmed by Wilmarth and Ishii [8] in vertical rectangular channels with gap widths of 1.0 and 2.0 mm for air–water two-phase flow. Within our experimental range the void fraction is predicted to be 0.72 using the following correlation proposed by Mishima and Hibika [9] developed in small diameter vertical tubes ($D = 1.0$–4.9 mm) for an air–water system:

$$\alpha = \frac{1}{1.2 + 0.51\exp(-691D)} \tag{2}$$

Finally the value of the dimensionless vapor flux for the transition is calculated to be 0.78 by Eq. (1) as shown by a vertical line in Fig. 6. This value is very close to 0.9 proposed by Wallis mentioned above. Comparing the experimental vapor flux with the predicted one, the flow regime might be annular except the entrance region below $Z = 10$ mm of the test section. Therefore, nucleate boiling in a liquid film or film evaporation without any boiling might be a predominant heat transfer regime in the tube.

In a two-phase flow the nucleate boiling is characterized by the presence of active nucleation sites on the heated wall and in the convective evaporation region heat transfer is controlled by the local liquid flow rate and film thickness. In the experiment, liquid flow rate cannot be measured since it is too small and difficult to detect with a pitot tube. Therefore, the liquid flow rate and film thickness are predicted by the following empirical film thickness correlation of Fukano and Furukawa [10], developed for a vertical gas–liquid annular flow regime:

$$\delta = 0.0594D\exp[-0.34(j_g/\sqrt{gD})^{0.25} \times (\rho_L j_l D/\mu_l)^{0.19} x^{0.6}] \tag{3}$$

In the equation, the liquid flow rate is required to obtain the liquid film thickness. Since in the present study a liquid flow rate measurement by a pitot tube in the downcomer is failed due to much lower pressure difference than 1 Pa in the pitot tube, the following correlation [11] of slip ratio, S, between vapor and liquid velocity is used to obtain the liquid flow rate:

$$S = \sqrt{\frac{\rho_l}{\rho_g}}\sqrt{\frac{\alpha}{2}} \tag{4}$$

Klimenko [12] considered the following convective number, N_{CB}, for the transition criterion between nucleate boiling and convective evaporation regions using the available data for water, freons, and cryogenics with

ranges: pressure 61–1480 kPa, mass flux 50–2690 kg/m^2 s, tube diameters 1.63–41.3 mm,

$$N_{CB} = (h_{fg}G/q)[1 + x(\rho_l/\rho_g - 1)](\rho_g/\rho_l)^{1/3} \quad (5)$$

and the transition criteria are: nucleate boiling $N_{CB} < 1.6 \times 10^4$ evaporation $N_{CB} > 1.6 \times 10^4$.

Fig. 7 demonstrates the classification of the obtained measured heat transfer coefficients into nucleate boiling and convective evaporation regions. In the figure NB and CV stand for nucleate boiling and convective evaporation into heat transfer regime, respectively. According to the transition criterion, all measured heat transfer coefficients are in the nucleate boiling regime. At other conditions, the results are similar to that shown in Fig. 7.

Fig. 8(a) and (b) presents the comparison of the measured average heat transfer coefficients with predictions by the pool boiling correlations of Stephan and Abdelsalam [4] and McNelly [13], respectively. The Stephan correlation covers a wide pressure range of 10–2660 kPa for R-113, which was confirmed by Wambsganss et al. [3] for boiling in a small diameter tube as mentioned in the introduction. McNelly developed the boiling correlation on the assumption that the main heat transfer resistance is concentrated in a thin liquid layer adjacent to the heated surface. The figures indicate that both correlations equally well predict the experimental data within an error of ±20%. Therefore, negligible enhancement in heat transfer is obtained although D/B is less than 1.5, which differs from the finding of Klimenko [2].

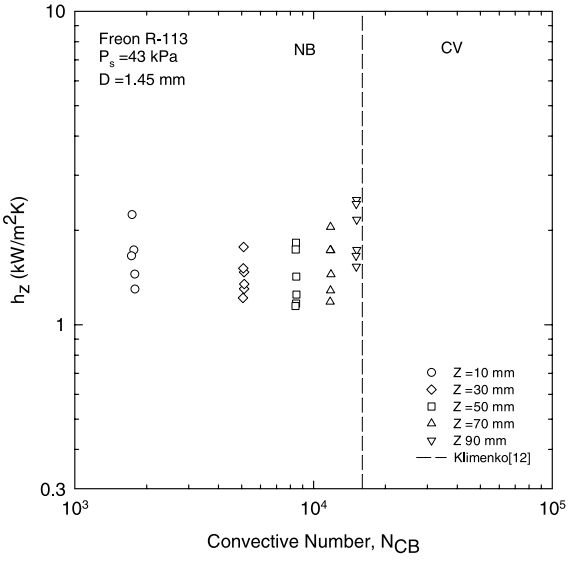

Fig. 7. Relationship between local heat transfer coefficients and predicted convective number of Klimenko [12].

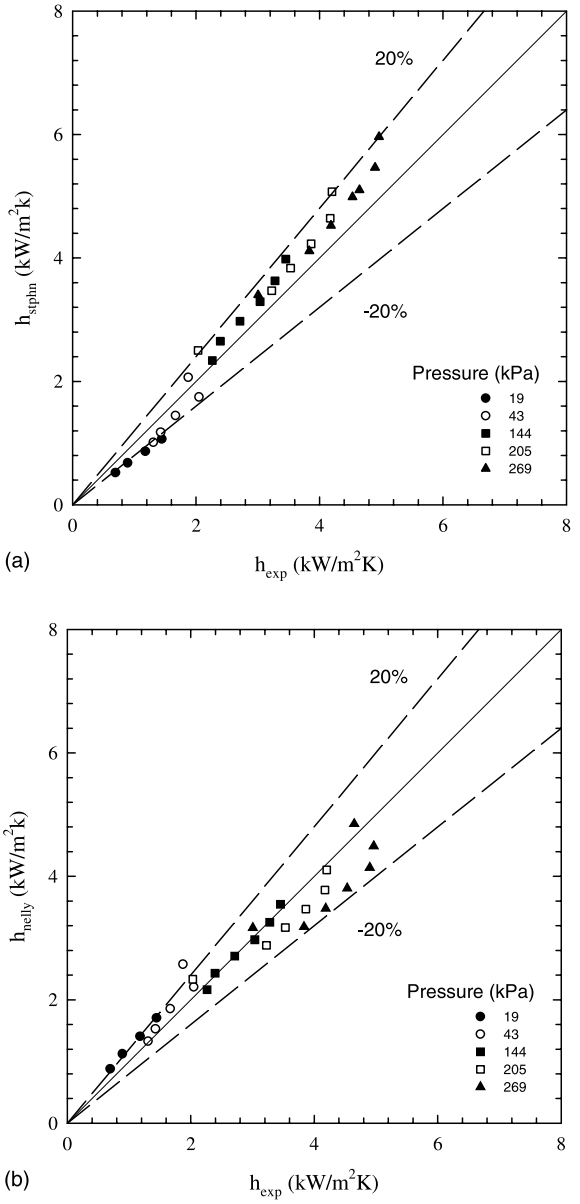

Fig. 8. Comparison of measured average heat transfer coefficients with predictions of Stephan–Abdelsalam [4] and McNelly [13].

5. Conclusions

Experimental investigation of boiling heat transfer in a small diameter tube at pressures below and above atmospheric gives the following results:

1. In consideration of measured vapor flux within the present experimental ranges, the flow regime is annular except the entrance region.

2. Boiling heat transfer enhancement is negligible within the experimental pressure range, which differs from the previous finding of Klimenko.
3. Comparisons of measured boiling heat transfer coefficients with existing pool boiling correlations of Stephan and Abdelsalam and McNelly indicate that both equally predict the experimental data within an error of $\pm 20\%$.

References

[1] E. Ishibashi, K. Nishikawa, Saturated boiling heat transfer in narrow spaces, Int. J. Heat Mass Transfer 12 (1969) 863–894.
[2] V.V. Klimenko, M.V. Fyodorov, Yu.A. Fomichyov, Channel orientation and influence on heat transfer with two-phase forced flow of nitrogen, Cryogenics 29 (1989) 31–36.
[3] M.W. Wambsganss, D.M. France, J.A. Jendrzejczyk, T.N. Tran, Boiling heat transfer in a horizontal small diameter tube, J. Heat Transfer 115 (1993) 963–972.
[4] K. Stephan, M. Abdelsalam, Heat transfer correlations for natural convection boiling, Int. J. Heat Mass Transfer 23 (1980) 73–87.
[5] M.B. Bowers, I. Mudawar, Two-phase electronic cooling using mini-channel and micro-channel heat sinks: Part 1 Design criteria and heat diffusion constraints, J. Electron. Packaging 116 (1994) 290–297.
[6] G.B. Wallis, Annular two-phase flow Part 1: A simple theory, J. Basic Eng. Trans. ASME (1970) 59–72.
[7] K. Mishima, M. Ishii, Flow regime transition criteria for upward two-phase flow in vertical tubes, Int. J. Heat Mass Transfer 27 (5) (1984) 723–737.
[8] T. Wilmarth, M. Ishii, Two-phase flow regimes in narrow rectangular vertical and horizontal channels, Int. J. Heat Mass Transfer 37 (12) (1994) 1749–1758.
[9] K. Mishima, T. Hibika, Some characteristics of air–water two-phase flow in small diameter vertical tubes, Int. J. Multiphase Flow 22 (4) (1996) 703–712.
[10] T. Fukano, T. Furukawa, Prediction of the effects of liquid viscosity on interfacial share stress and frictional pressure drop in vertical upward gas–liquid annular flow, in: M. Giot, F. Mayinger, G.P. Celata (Eds.), Experimental Heat Transfer, Fluid Mechanics and Thermodynamics, Edizioni ETS (1997) 1161–1168.
[11] S. Levy, Steam-slip theoretical prediction from momentum model, J. Heat Transfer (1960) 113–124.
[12] V.V. Klimenko, A generalized correlation for two-phase forced flow heat transfer, Int. J. Heat Mass Transfer 31 (3) (1988) 541–552.
[13] M.J. McNelly, A correlation of the rates of heat transfer to nucleate boiling liquids, J. Imperial College, Eng. Soc. 7 (1953) 18–34.